EPJ Web of Conferences **70**, 00079 (2014)
DOI: 10.1051/epjconf/ 20147000079

Charmless B decays

Aurélien MARTENS[1,a] on behalf of the LHCb Collaboration

[1] *LPNHE, Université Pierre et Marie Curie, Université Paris Diderot, CNRS/IN2P3, Paris, France.*

Abstract. During 2011, LHCb has collected an integrated luminosity of 1.1 fb^{-1}, giving rise to a large variety of measurements. Amongst these, measurements of *CP* violation in B decays play a central role. In particular *CP* violation measurements in charmless transitions of B mesons are of interest since they provide new or improved constraints on new physics contributions. These proceedings concentrate on LHCb results made public in the first half of the year 2012.

1 Introduction

The LHCb detector [1] is a single arm spectrometer designed to accurately measure decay products of B and D mesons for precision measurements at the LHC. In the following an overview of recent studies in charmless and radiative B decays performed by the LHCb collaboration is presented. Other measurements conducted with the LHCb detector are summarized in [2–4]. The commissioning of the detector and the performance reached with the current data are summarized in [5] while prospects for an upgraded LHCb detector are discussed in [6].

Key ingredients for the analyses presented in the following are the ability to trigger on and to disentangle different modes owing to dedicated ring-imaging Cherenkov detectors. Some channels of interest additionally require (or will require on longer term analyses) good tagging capabilities and excellent proper time resolution, that are detailed elsewhere [7]. The data samples used for the analyses presented here are based on pp collision data collected in 2011 at $\sqrt{s} = 7\,\text{TeV}$ correspond to integrated luminosities ranging from $0.35\,\text{fb}^{-1}$ to $1.0\,\text{fb}^{-1}$.

2 Two body charmless B decays

2.1 General strategy

CP violation in charmless B decays allows to extract information on the *CP* violating phases of the Unitarity Triangle β and γ. These measurements are generally sensitive to new physics effects, since the involved processes are characterized by dominant loop contributions. The drawback lies in the numerous diagram topologies that contribute to these decays. Thus the extraction of the weak phases is considered as more complicated than in the Standard Model benchmark measurements of these quantities performed with $B^0 \to J/\psi\, K^0_S$ open charm decays.

[a] e-mail: aurelien.martens@lpnhe.in2p3.fr

For instance, the $B \to hh'$ decays are key channels at LHCb to develop this strategy [8]. Tagged time dependent analyses are also targeted to maximally exploit the information contained in these decays.

2.2 First evidence for *CP* violation in the B_s^0 system

Searches for direct *CP* violation in the flavour specific $B^0_{(s)} \to K\pi$ decays are performed using an integrated luminosity of $0.35\,\text{fb}^{-1}$. Small corrections to the raw *CP* asymmetries, clearly visible by eye on Fig. 1, are introduced to account for detection and production asymmetries. Detection asymmetries, induced by different reconstruction efficiencies and by different cross sections in the interactions of oppositely charged particles with the detector material, are determined by means of large samples of two-body D meson decays. The former contribution amounts to about 0.2% and is further cancelled owing to the ability to flip the magnetic field in LHCb. The latter is dominated by the kaon detection asymmetry and amounts to about 1%. The production asymmetry of B^0 mesons is estimated using $B^0 \to J/\psi K^{*0}$ decays, assuming absence of *CP* violation. This asymmetry is further diluted by the mixing of the B^0 mesons and the shape of the proper time acceptance. Owing to the fast B_s^0 oscillations, the possible presence of a B_s^0 production asymmetry plays no role. The total correction from these polluting asymmetries amounts to $1.0 \pm 0.2\%$ and $-0.7 \pm 0.6\%$ respectively in the B_s^0 and B^0 cases.

B_s^0 and B^0 *CP*-violating asymmetries are thus determined to be [9]:

$$A_{CP}^{B_s^0 \to K\pi} = \frac{\mathcal{B}\left(\bar{B}_s^0 \to K^+\pi^-\right) - \mathcal{B}\left(B_s^0 \to K^-\pi^+\right)}{\mathcal{B}\left(\bar{B}_s^0 \to K^+\pi^-\right) + \mathcal{B}\left(B_s^0 \to K^-\pi^+\right)} = 0.27 \pm 0.08\ (\text{stat.}) \pm 0.02\ (\text{syst.}), \quad (1)$$

$$A_{CP}^{B^0 \to K\pi} = \frac{\mathcal{B}\left(\bar{B}^0 \to K^-\pi^+\right) - \mathcal{B}\left(B^0 \to K^+\pi^-\right)}{\mathcal{B}\left(\bar{B}^0 \to K^-\pi^+\right) + \mathcal{B}\left(B^0 \to K^+\pi^-\right)} = -0.088 \pm 0.011\ (\text{stat.}) \pm 0.008\ (\text{syst.}). \quad (2)$$

For the first time, an evidence of *CP* violation in the B_s^0 system is obtained and for the first time at an hadron collider a direct *CP* asymmetry is observed with a significance exceeding 5σ. The dominating systematics are linked to the modeling of the B invariant mass in the B_s^0 case and to the polluting asymmetries in the B^0 case. Both will be reduced with larger integrated luminosities. These results are in agreement and more precise with respect to previous measurements made by BABAR [10], BELLE [11] and CDF [12].

2.3 Branching fraction measurements of $B \to hh'$ decays

With $0.37\,\text{fb}^{-1}$, the rare $B^0 \to K^+K^-$ and $B_s^0 \to \pi^+\pi^-$ decay modes, dominated by exchange and penguin annihilation diagrams, are searched for [13]. The first observation for $B_s^0 \to \pi^+\pi^-$ is obtained and its branching fraction measured to be

$$\mathcal{B}\left(B_s^0 \to \pi^+\pi^-\right) = (0.95\ ^{+0.21}_{-0.17}\ (\text{stat.}) \pm 0.13\ (\text{syst.})) \times 10^{-6}, \quad (3)$$

while the $B^0 \to K^+K^-$ branching fraction is found equal to

$$\mathcal{B}\left(B^0 \to K^+K^-\right) = (0.11\ ^{+0.05}_{-0.04}\ (\text{stat.}) \pm 0.06\ (\text{syst.})) \times 10^{-6}. \quad (4)$$

These measurements allow to assert the size of the pollution coming from these diagrams in the extraction of the *CP* violating observables. In the same analysis the $B_s^0 \to K^-\pi^+$ branching fraction is determined,

$$\mathcal{B}\left(B_s^0 \to K^-\pi^+\right) = (5.4 \pm 0.4\ (\text{stat.}) \pm 0.6\ (\text{syst.})) \times 10^{-6}, \quad (5)$$

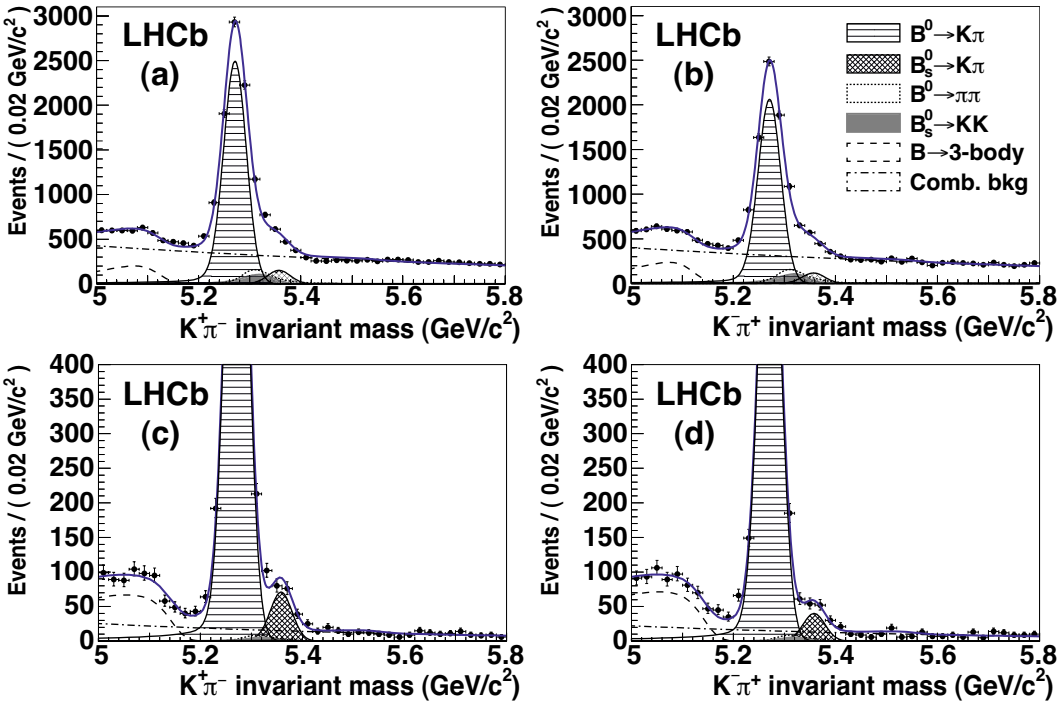

Figure 1. The $K^+\pi^-$ (left) and $K^-\pi^+$ (right) invariant mass spectra optimized for the B^0 asymmetry measurement (top), and for the B_s^0 asymmetry measurement (bottom), see [9] for details.

with the best precision to date. The ratio of branching fractions of similar Λ_b decays is also extracted,

$$\mathcal{B}(\Lambda_b \to pK^-)/\mathcal{B}(\Lambda_b \to p\pi^-) = 0.86 \pm 0.08 \text{ (stat.)} \pm 0.05 \text{ (syst.)}. \quad (6)$$

2.4 Time dependent *CP* violation measurements of $B \to hh'$ decays

With an updated sample up to $0.69\,\text{fb}^{-1}$, the analysis is sensitive to time dependent *CP* violation [14], that is measured by means of opposite side flavour tagging, based on a combination of the electron, muon, kaon and secondary vertex taggers, which exploit the decay products of the other b-hadron produced in the event [7]. In order to calibrate this algorithm, and to exercise the whole analysis, $B^0 \to K^+\pi^-$ is used as a proxy.

From a simultaneous fit of the $K\pi$ invariant mass and the time of flight of the reconstructed B meson, and assuming the B_s^0 mixing parameters are perfectly determined by other LHCb measurements [16, 17] and $\Delta\Gamma_d = 0$, the effective tagging efficiency (or *tagging power*) $\varepsilon D^2 = 2.3 \pm 0.1\%$, the B^0 and B_s^0 production asymmetries $A_P(B^0) = -0.015 \pm 0.013$ and $A_P(B_s^0) = -0.03 \pm 0.06$, can be extracted together with $\Delta m_d = 0.484 \pm 0.019\,\text{ps}^{-1}$ and $\tau_B = 1.509 \pm 0.011$ ps, where only statistical uncertainties are quoted. The last two measurements, which provide a cross-check of the analysis, are in good agreement with the world averages [18]. Fig. 2 shows the time dependent mixing asymmetry for events lying in the invariant mass window $[5.20, 5.32]$ GeV. The first three quantities are used as input for the $B^0 \to \pi^+\pi^-$ and $B_s^0 \to K^+K^-$ time dependent analyses.

In order to extract the time dependent violation in $B^0 \to \pi^+\pi^-$ decays, Δm_d is fixed to the central value measured in another LHCb analysis [15] that provides $\Delta m_d = 0.499 \pm 0.032\,(\text{stat.}) \pm 0.003\,(\text{syst.})\ \text{ps}^{-1}$, the central value being varied to estimate the related systematic uncertainty. Assuming $\Delta\Gamma_d = 0$, the direct and mixing induced *CP* asymmetries are both extracted together with their statistical correlation factor:

$$A^{dir.}_{\pi^+\pi^-} = 0.11 \pm 0.21\,(\text{stat.}) \pm 0.03\,(\text{syst.}), \tag{7}$$

$$A^{mix.}_{\pi^+\pi^-} = -0.56 \pm 0.17\,(\text{stat.}) \pm 0.03\,(\text{syst.}), \tag{8}$$

$$\rho(A^{dir.}_{\pi^+\pi^-}, A^{mix.}_{\pi^+\pi^-}) = 0.34\,(\text{stat.}). \tag{9}$$

The dominating sources of (relatively small) systematic uncertainties are the central values used for the input parameters (namely Δm_d and tagging efficiencies) and the model used to parameterize the decay time (both signal and background). The raw mixing asymmetry together with the result of the fit is shown on Fig. 3 (left).

Time dependent *CP* violation is also looked for in $B^0_s \to K^+K^-$ decays by fixing $\Delta m_s = 17.63 \pm 0.11\,(\text{stat.}) \pm 0.02\,(\text{syst.})\ \text{ps}^{-1}$ [16] and $\Gamma_s = 0.657 \pm 0.009\,(\text{stat.}) \pm 0.008\,(\text{syst.})\ \text{ps}^{-1}$ [17] to their respective central values, allowing for a determination of $\Delta\Gamma_s = 0.076 \pm 0.019\,\text{ps}^{-1}$ as a side product of the analysis, where only statistical uncertainty is quoted. This is in agreement with a previous measurement of the same quantity by another LHCb analysis [17], with similar uncertainty and thus consists in a suitable cross-check. The direct and mixing induced *CP* asymmetries are both extracted together with their statistical correlation factor:

$$A^{dir.}_{K^+K^-} = 0.02 \pm 0.18\,(\text{stat.}) \pm 0.04\,(\text{syst.}), \tag{10}$$

$$A^{mix.}_{K^+K^-} = 0.17 \pm 0.18\,(\text{stat.}) \pm 0.05\,(\text{syst.}), \tag{11}$$

$$\rho(A^{dir.}_{K^+K^-}, A^{mix.}_{K^+K^-}) = 0.10\,(\text{stat.}), \tag{12}$$

where the contributions to the systematic uncertainties are again dominated by the uncertainy on the input parameters and the decay time model. The raw mixing asymmetry together with the result of the fit is shown on Fig. 3 (right).

Hence a first measurement of the time dependent asymmetry in $B^0_s \to K^+K^-$ decays is obtained, as well as an evidence of mixing-induced *CP* violation in the $B^0 \to \pi^+\pi^-$ decays. This last result is in agreement with previous determinations but it does not yet reach their precision [10, 19]. This analysis may be improved in the future by means of the addition of the same side tagging algorithms under study at LHCb.

2.5 Effective lifetime measurement of the B^0_s meson in the $B^0_s \to K^+K^-$ decay

A new analysis of the effective lifetime of the B^0_s meson in the $B^0_s \to K^+K^-$ decay is performed with $1\,\text{fb}^{-1}$. This quantity, sensitive to *CP* violation and potential new physics effects, has already been measured at LHCb [20], but suffers from a lack of knowledge on the decay time acceptance. Thus a strategy aiming at flattening the decay time acceptance at each stage of the analysis, including the trigger, and thus reducing the related systematic uncertainty, is developed [21]. The acceptance of the reconstructed B^0_s candidates as a function of the decay time is shown on Fig. 4. The result of the analysis

$$\tau_{KK} = 1.468 \pm 0.046\,(\text{stat.}) \pm 0.006\,(\text{syst.})\ \text{ps}, \tag{13}$$

for which the systematic uncertainty is still dominated by a proper time reconstruction bias, is in agreement with the Standard Model prediction $\tau_{KK} = 1.390 \pm 0.032$ [22].

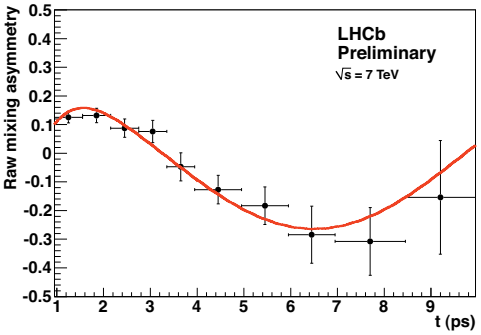

Figure 2. Raw mixing asymmetry in the $B^0 \to K^+\pi^-$ signal mass region with the result of the fit overlaid [14].

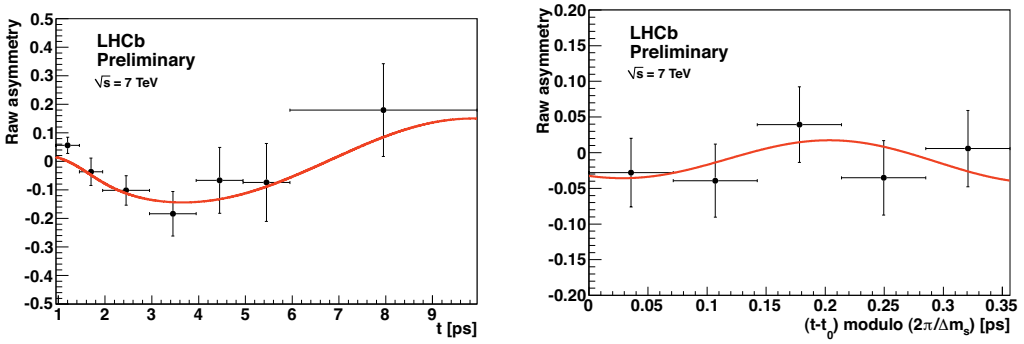

Figure 3. Raw mixing asymmetry in the $B^0 \to \pi^+\pi^-$ and $B_s^0 \to K^+K^-$ signal mass regions respectively on the left and right hand side of the figure, with the result of the fit overlaid [14].

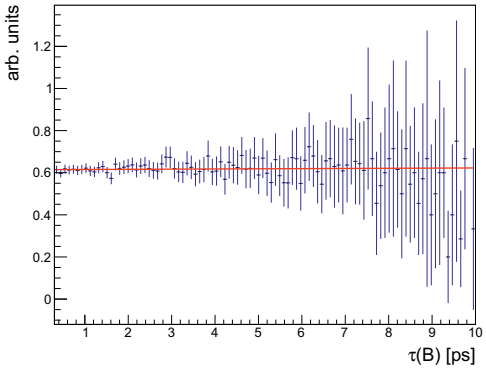

Figure 4. Acceptance of B mesons as a function of the decay time on simulated $B_s^0 \to K^+K^-$ signal candidates. A linear fit to the acceptance versus decay time yields a slope of $0.0008 \pm 0.0034\,\mathrm{ps}^{-1}$ [21].

3 Charmless B decays to two vector mesons

Triple product asymmetries are measured in the $B_s^0 \to \phi\phi$ decay. These asymmetries, sensitive to *CP*-violation under the assumption that *CPT* is conserved, are measured with $1\,\text{fb}^{-1}$ together with polarization amplitudes parameters [23], see Fig. 5:

$$|A_0|^2 = 0.365 \pm 0.022\ (\text{stat.}) \pm 0.012\ (\text{syst.}), \tag{14}$$

$$|A_\perp|^2 = 0.291 \pm 0.024\ (\text{stat.}) \pm 0.010\ (\text{syst.}), \tag{15}$$

$$\cos(\delta_\parallel) = -0.844 \pm 0.068\ (\text{stat.}) \pm 0.029\ (\text{syst.}), \tag{16}$$

$$A_U = \frac{N(U<0) - N(U>0)}{N(U<0) + N(U>0)} = -0.055 \pm 0.036\ (\text{stat.}) \pm 0.018\ (\text{syst.}), \tag{17}$$

$$A_V = \frac{N(V<0) - N(V>0)}{N(V<0) + N(V>0)} = +0.010 \pm 0.036\ (\text{stat.}) \pm 0.018\ (\text{syst.}), \tag{18}$$

where $U = \frac{1}{2}\sin(2\Phi)$, $V = \sin(\varepsilon\Phi)$ and $\varepsilon = \text{sign}(\cos\theta_1 \cos\theta_2)$, Φ being the angle between the decay planes of the two ϕ mesons and $\cos\theta_{1,2}$ the helicity angles in the two ϕ meson decays. Systematic uncertainties on the triple product asymmetries are dominated by angular and decay time acceptances while the systematic uncertainty on the S wave component additionally contributes significantly in the determination of the polarization amplitudes. This result is in agreement with a previous existing CDF measurement [24]. On the longer term, this channel may also be used for the determination of the mixing phase in the B_s^0 system ϕ_s.

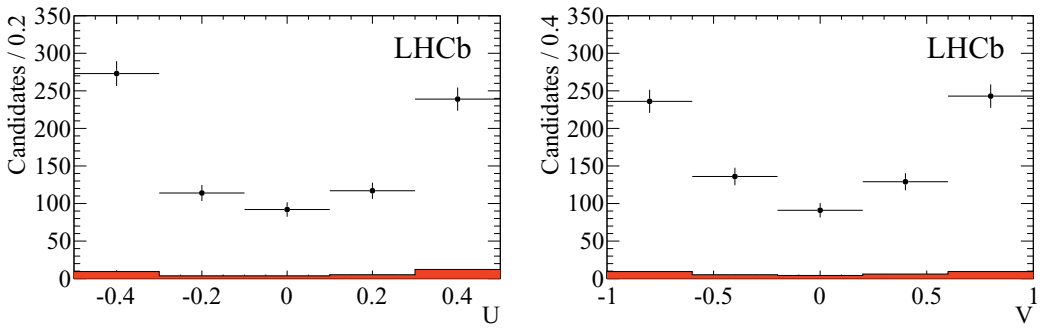

Figure 5. Distributions of the U (left) and V (right) observables for the $B_s^0 \to \phi\phi$ data in the mass range $5286.6 < m(B_s^0) < 5446\,\text{MeV}$. The distribution for the background is taken from the mass sidebands, normalized to the same mass range and is shown by the solid histogram [23].

4 Radiative charmless B decays

$B^0 \to K^{*0}\gamma$ and $B_s^0 \to \phi\gamma$ decays are of interest since they proceed through penguin transitions in which sizeable new physics effects can be introduced. Recent LHCb measurements are summarized below.

4.1 Ratio of branching fractions measurement

With an integrated luminosity of $0.37\,\text{fb}^{-1}$, the $B^0 \to K^{*0}\gamma$ and $B_s^0 \to \phi\gamma$ decay modes are reconstructed with the LHCb detector with a resolution of approximately 100 MeV, achieved thanks to an

excellent calibration of the calorimeter energy at the level of 1 to 2 %. Approximately 1700 and 240 signal candidates are respectively reconstructed in $B^0 \to K^{*0}\gamma$ and $B_s^0 \to \phi\gamma$, as shown in Fig. 6. In this analysis the background is simply modeled by a falling exponential in both decay modes.

The ratio of branching fractions is thus measured [25]:

$$\frac{\mathcal{B}\left(B^0 \to K^{*0}\gamma\right)}{\mathcal{B}\left(B_s^0 \to \phi\gamma\right)} = 1.12 \pm 0.08\ (\text{stat.})\ ^{+0.06}_{-0.04}\ (\text{syst.})\ ^{+0.09}_{-0.08}\ (f_s/f_d), \tag{19}$$

where the ratio of fragmentation fractions is determined by an independent LHCb analysis [26, 27]. The dominating systematic uncertainties come from the calibration of the particle identification efficiencies and the model used for the background. This result is in good agreement with the Standard Model that predicts a ratio equal to unity, within 20% of relative uncertainty [28].

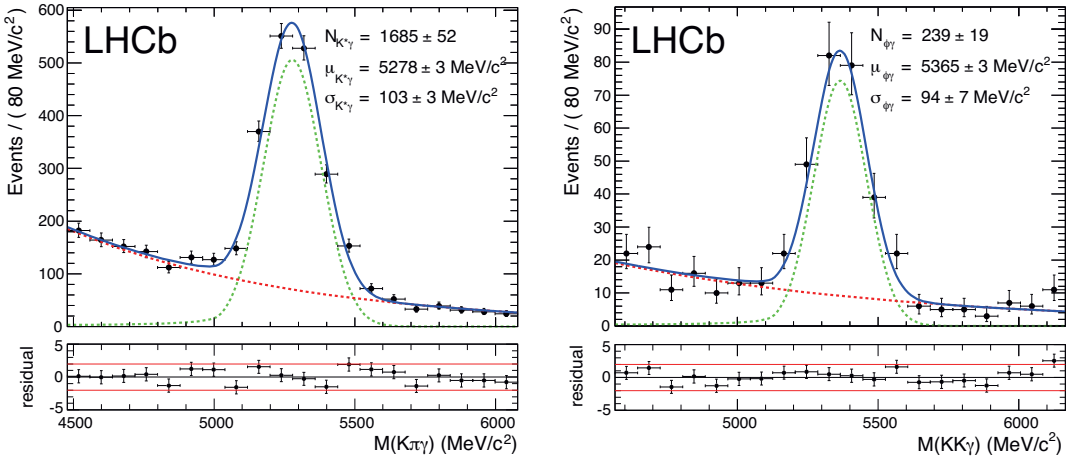

Figure 6. Result of the fit for the $B^0 \to K^{*0}\gamma$ (left) and $B_s^0 \to \phi\gamma$ (right). The black points represent the data and the fit result is represented as a solid line. The signal is fitted with a Crystal Ball function (light dashed line) and the background is described as an exponential (dark dashed line), see [25] for details.

4.2 $B^0 \to K^{*0}\gamma$ *CP* asymmetry measurement

Since the modeling of the background under the signal peaks was found to be a limiting systematic uncertainty in the previous analysis, it is refined for the *CP* violation measurement. By order of relative importance, the following specific backgrounds are considered: $B^{\pm,0} \to K^{*0}\pi^{\pm,0}\gamma$, $B^0 \to K^{*0}\pi^0 X$, $B_s^0 \to K^{*0}\gamma$, $\Lambda_b \to \Lambda^*\gamma$, $B^0 \to K^+\pi^-\pi^0$ and $B_s^0 \to K^-\pi^+\pi^0$. In particular the combinatorial background yields and shapes in the two flavour final states are left free in the fit, as it can be observed in Fig. 7.

The time integrated *CP* asymmetry

$$A_{CP} = 0.008 \pm 0.017\ (\text{stat.}) \pm 0.009\ (\text{syst.}) \tag{20}$$

is measured [29]. However the dominant systematic contribution is coming from the asymmetry of the background, that enters as a correction in the extraction of the asymmetry. This preliminary result is in good agreement with the Standard Model prediction [30] and with the BABAR measurement [31].

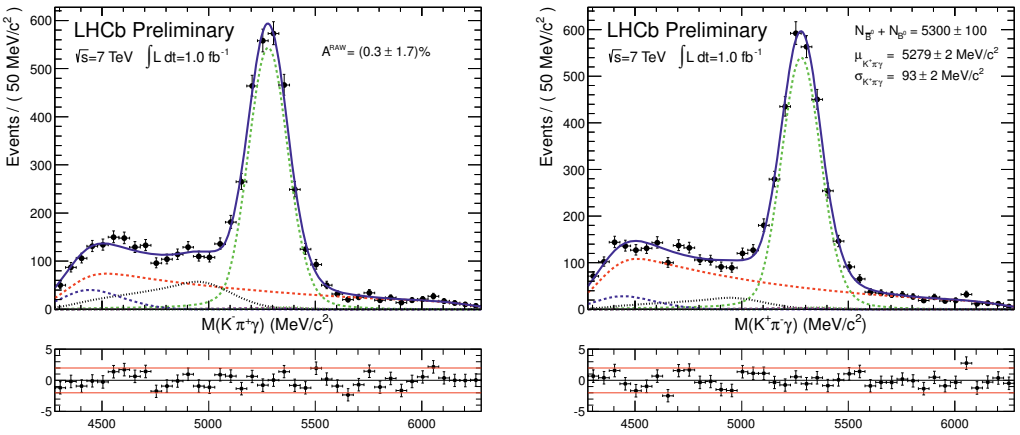

Figure 7. Simultaneous fit $B^0 \to K^{*0}\gamma$ (left) and $\bar{B}^0 \to \bar{K}^{*0}\gamma$ (right). The black points represent the data and the fit result is represented as a solid blue line. The signal is fitted with a double-sided Crystal Ball function (dashed green line). The generic combinatorial background is modelled with an exponential function (dashed red lines).$B^{\pm,0} \to K^{*0}\pi^{\pm,0}\gamma$ and $B^0 \to K^{*0}\pi^0 X$ backgrounds are respectively also shown (dotted black and dashed blue lines respectively), see [29] for details.

5 Conclusion

In the beginning of 2012 new results on charmless and radiative charmless B decays have been obtained by LHCb. Time dependent CP violation in $B_s^0 \to K^+K^-$ decays is constrained for the first time. Effective lifetime measurements are pursued in the same decay with various approaches, and most recently using a method that aims at flattening decay time acceptance. World leading measurement of the triple product asymmetries in $B_s^0 \to \phi\phi$ is obtained together with a first measurement of the polarization amplitudes in this decay. World leading measurements of the branching fraction of the $B_s^0 \to \phi\gamma$ decay is obtained together with a world leading measurement of the CP asymmetry in $B^0 \to K^{*0}\gamma$.

All these measurements, obtained with at most $1\,\text{fb}^{-1}$ of integrated luminosity, are compatible with Standard Model predictions. Further results are expected to appear especially with three body and two vector meson charmless B decays.

Aknowledgements

I would like to thank the organizers for their hospitality and the chance to visit one of the most beautiful, and laden with history, places in the Mediterranean basin.

References

[1] Alves, A. Augusto Jr and others, LHCb Collaboration, JINST **3**, (2008) S08005
[2] Lopez March N., these proceedings
[3] Sciascia B., these proceedings
[4] Contu A., these proceedings

[5] Egede U., these proceedings
[6] Hopchev P., these proceedings
[7] Aaij, R and others, LHCb Collaboration, Eur. Phys. J. **C72**, (2012) 2022
[8] Adeva, B. and others, LHCb Collaboration, arXiv **hep-ex**, (2009) 0912.4179
[9] Aaij, R and others, LHCb Collaboration, Phys. Rev. Lett. **108**, (2012) 201061
[10] Aubert, B. and others, BaBar Collaboration, arXiv **hep-ex**, (2008) 0807.4226
[11] Chang, P., on behalf the Belle Collaboration, PoS **EPS-HEP2011**, (2011) 140
[12] Aaltonen, T. and others, CDF Collaboration, Phys. Rev. Lett **106**, (2011) 181802
[13] Aaij, R. and others, LHCb Collaboration, arXiv **hep-ex**, (2012) 1206.2794
[14] LHCb Collaboration, LHCb-CONF-2012-007
[15] LHCb Collaboration, LHCb-CONF-2011-010
[16] Aaij, R. and others, LHCb Collaboration, Phys. Lett. **B709**, (2012) 177
[17] Aaij, R. and others, LHCb Collaboration, arXiv **hep-ex**, (2011) 1112.3183
[18] Amhis, Y. and others, Heavy Flavour Averaging Group, arXiv **hep-ex**, (2012) 1207.1158
[19] Ishino, H. and others, Belle Collaboration, Phys. Rev. Lett. **98**, (2007) 211801
[20] Aaij, R. and others, LHCb Collaboration, Phys. Lett. **B707**, (2012) 349
[21] LHCb Collaboration, LHCb-CONF-2012-001
[22] Fleischer, R. and Knegjens, R., Eur. Phys. J. **C71**, (2011) 1532
[23] Aaij, R. and others, LHCb Collaboration, arXiv **hep-ex**, (2012) 1204.2813
[24] Aaltonen, T. and others, CDF Collaboration, Phys. Rev. Lett. **107**, (2011) 261802
[25] Aaij, R. and others, LHCb Collaboration, arXiv **hep-ex**, (2012) 1202.6267
[26] Aaij, R. and others, LHCb Collaboration, Phys. Rev. Lett. **107**, (2011) 211801
[27] Aaij, R. and others, LHCb Collaboration, Phys. Rev. **D85**, (2012) 032008
[28] Ali, A. and Pecjak, B. D. and Greub, C., Eur. Phys. J. **C55**, (2008) 577
[29] LHCb Collaboration, LHCb-CONF-2012-004
[30] Keum, Y.Y. and Matsumori, M. and Sanda, A.I., Phys. Rev. **D72**, (2005) 014013
[31] Aubert, B. and others, BABAR Collaboration, Phys. Rev. Lett. **103**, (2009) 211802